Robotic Force Control using Observer-based Strict Positive Real Impedance Control

Johansson, Rolf; Robertsson, Anders

Published in:
Proceedings. ICRA '03.

DOI:
10.1109/ROBOT.2003.1242162

2003

Proceedings of the 2003 IEEE
International Conference on Robotics & Automation
Taipei, Taiwan, September 14-19, 2003

Robotic Force Control using Observer-based Strict Positive Real Impedance Control

Rolf Johansson and Anders Robertsson

Department of Automatic Control
Lund Institute of Technology, Lund University
PO Box 118, SE-221 00 Lund, Sweden
Phone +46 46 222 8791, Fax +46 46 138118
E-mail: Rolf.Johansson@control.lth.se, Anders.Robertsson@control.lth.se

***Abstract*—This paper presents theoretical and experimental results on observer-based impedance control for force control without velocity feedback. As the velocity may not available to measurement, which is often the case for industrial robots, an observer was designed to reconstruct velocity in such a way that it be useful for stabilizing feedback control and to modification of the damping in the impedance relationship. A good model of the robot joint used was obtained by system identification. Experiments were carried out on an ABB industrial robot 2000 to demonstrate results on observer-based SPR feedback applied in the design. Stability was shown via a modified Popov criterion.**

Keywords: Impedance control, Observers, Stability, Popov criterion, Robotics.

I. INTRODUCTION

Today industrial robots are used in a wide range of applications. Many of these applications will naturally require the robot to come into contact with a physical environment—*e.g.*, welding, grinding, and drilling. This interaction with the environment will set constraints on the geometric paths that can be followed, a situation referred to as constrained motion.

To avoid excessive contact forces the robot trajectory must be planned with high accuracy. This is, however, often impossible because of geometric uncertainty and finite positioning accuracy. A way to solve this conflict is to let the robot manipulator be force controlled—*e.g.*, impedance control control and hybrid force/position control [21].

Among robot force control methods used, impedance control is aimed at control of the dynamic relation between position error and force error in interaction similar to Newton's second law of motion [9], [13], [2], [21]. The impedance relationship between force F and position x used in this paper is represented by the equation

$$F = K \cdot x + D \cdot \dot{x} \tag{1}$$

where the positive constants K and D represent design parameters for stiffness and damping, respectively. One way to achieve this relation is to control the following impedance variable to zero

$$\begin{aligned} z(t) &= Kx(t) + D\dot{x}(t) - F(t), \\ Z(s) &= (K + sD)X(s) - F(s) \end{aligned} \tag{2}$$

In its simplest form, such control can be accomplished using an ordinary PI-controller which involves feedback of z. A problem, however, is that the velocity is often not available for measurement and that differentiating feedback is error prone. Although stability and robustness may be improved using more sophisticated model-based control, poor force impact models and other aspects of insufficient world modeling still constitute a challenge to model-based force control [13], [2], [21].

This paper presents a method to improve impedance control by means observer-based feedback in one dimension [20], [8]. Our approach is based on strict positive real or feedback positive real (SPR/FPR) observer-based feedback design with a modified Popov criterion used for the stability analysis. In Sec. II, the control law and the design procedure are described and Sec. II is devoted to the stability analysis. Sections IV and V describe the experimental setup and the identification of a model for the system. Simulations and an experiment are presented in Sec. VI followed by a discussion and conclusions.

II. THE CONTROL LAW

Molander and Willems provided a design procedure for L—i.e., design for nonlinear state-feedback control—with specified gain margin [17]. They made a characterization of the conditions for stability of feedback systems with a high gain margin

$$\dot{x} = Ax + Bu, \quad z = Lx, \quad u = -f(z,t) \tag{3}$$

with $f(\cdot,\cdot)$ enclosed in a sector $[K_1, K_2]$. The following procedure was suggested to find a state-feedback vector L such that the closed-loop system will tolerate any

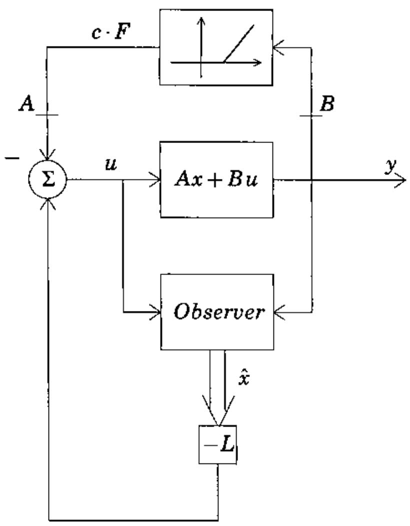

Fig. 1. Block diagram of the impedance control. The Popov plot of the transfer function from A to B is used to analyze stability for the contact force nonlinearity.

$f(\cdot,\cdot)$ enclosed in a sector $[K_1, K_2]$. Synthesis of a state-feedback vector L with a robustness sector $[K_1, \infty)$ follows from

- Pick a matrix $Q = Q^T > 0$ such that (A, Q) is observable;
- Solve the Riccati equation $PA + A^T P - 2K_1 PBB^T P + Q = 0$ and take $L = B^T P$

which can be recognized as an FPR condition [15]—i.e., the stability condition will be that of an SPR condition on $L(sI - A + K_1 BL)^{-1}B$. The design procedure was based on a circle-criterion proof and involved a solution of a Riccati equation. In the context of observer-based state feedback control, the controllability condition presents a problem of application. In [12], such SPR/FPR design has been generalized to the case of observer-based state feedback control.

Strict Positive Real Design

Now consider the state feedback control law

$$u = -L\hat{x} - cF \tag{4}$$

where F is the measured contact force and c is a constant. The state estimates, $\hat{x}$, are given by the full-order observer

$$\dot{\hat{x}}(t) = A\hat{x}(t) + Bu(t) + K_f(y(t) - C\hat{x}(t)) \tag{5}$$

where the observer gain, K_f, is chosen using ordinary pole-placement of the eigenvalues of $A - K_f C$, with the system matrices (A, C) given by (15).

The control law (4) is equivalent to proportional control of the output variable (2), since the states in the state-space model of the robot joint are position and velocity.

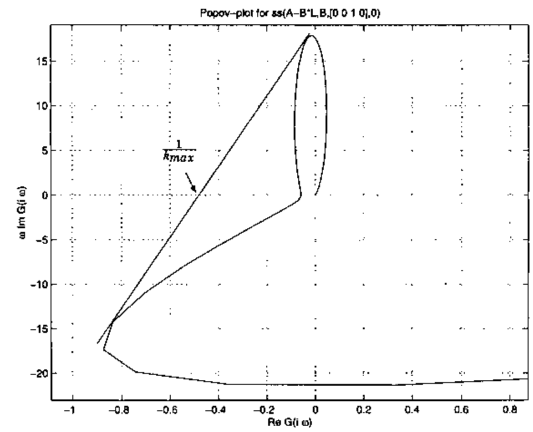

Fig. 2. Popov plot for the transfer function from A to B in Fig. 1 for the example. The maximum slope of the nonlinearity is given by k_{max}. For the quite compliant environment used in the experiments the stability margin is large.

The state feedback matrix, L, is chosen according to the results in [12], i.e.,

$$L = R^{-1}B^T P_c, \quad P_c = P_c^T > 0 \tag{6}$$

where P_c is the solution to the Riccati equation

$$P_c(A - BL) + (A - BL)^T P_c = -Q_c - P_c B R^{-1} B^T P_c \tag{7}$$

$Q_c > 0$ and $R > 0$ are design matrices, which represent penalties on the states and the control signal, respectively. The stiffness and damping in the impedance relation are modified indirectly by the choice of the state penalty matrix, Q_c, which is chosen as

$$Q_c = \begin{bmatrix} K_p & 0 & 0 & 0 \\ 0 & D_p & 0 & 0 \\ 0 & 0 & 0.01 & 0 \\ 0 & 0 & 0 & 0.01 \end{bmatrix} \tag{8}$$

The penalty, K_p, on the position will affect the stiffness in the impedance relation, whereas D_p will affect the damping.

III. Stability Analysis

Stability concerning the contact force nonlinearity is analyzed using the Popov criterion. A block diagram of the system under the impedance control (4) is shown in Fig. 1. Stability is analyzed by plotting the Popov curve for the transfer function from A to B. Then it is possible to determine a sector $[0, k_{max}]$ in which the contact force nonlinearity must be contained in order to guarantee stability [14]. The stability sector will be affected by the choice of the state feedback L.

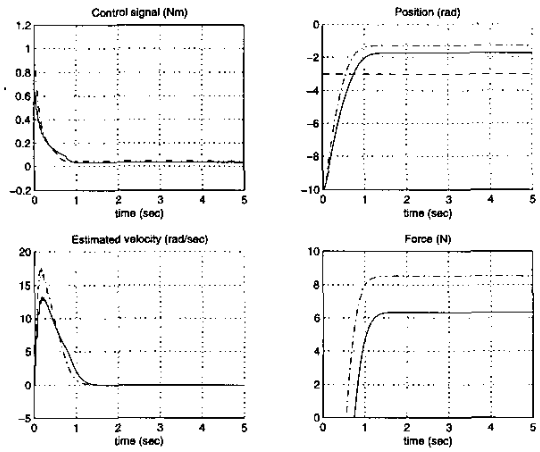

Fig. 3. Simulation of observer-based impedance control for two different choices of the penalty K_p. The solid curve corresponds to $K_p = 5$ and the dash-dotted to $K_p = 10$. The dashed line in the position plot marks the location of the screen. It is seen that a larger K_p gives higher stiffness, leading to a larger contact force. $D_p = 1$ in both simulations.

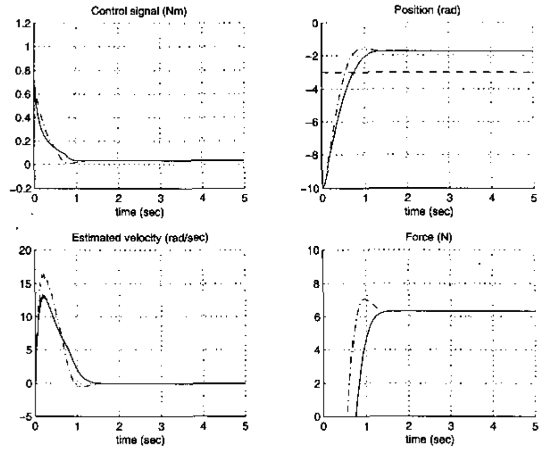

Fig. 4. Simulation of observer-based impedance control for two different choices of the penalty D_p. The solid curve corresponds to $D_p = 1$ and the dash-dotted to $D_p = 0.1$. The dashed line in the position plot marks the location of the screen. It is seen that a larger D_p increases the damping during the transient. $K_p = 5$ in both simulations.

Example In the design, the following matrices have been used

$$Q_c = \begin{bmatrix} 10 & 0 & 0 & 0 \\ 0 & 1 & 0 & 0 \\ 0 & 0 & 0.01 & 0 \\ 0 & 0 & 0 & 0.01 \end{bmatrix}, \quad R = 1000 \tag{9}$$

resulting in the state feedback gain

$$L = \begin{bmatrix} -0.0795, & 0.0191, & 0.1796, & 0.0054 \end{bmatrix} \tag{10}$$

The observer gain matrix, K_f, was chosen as

$$K_f = \begin{bmatrix} 270, & 16700, & 78, & -1190 \end{bmatrix}^T \tag{11}$$

Fig. 2 shows the Popov plot of the transfer function from A to B in Fig. 1 using the gain matrices above. To guarantee stability the slope of the nonlinearity, i.e., $c \cdot k$, must be less than $|k_{max}|$. The stiffness of the environment is $k = 5$ N/rad as mentioned in Sec. IV and $c = 0.01$. From Fig. 2, it can be concluded that the stability margin is large in this case.

IV. Experimental Set-up

The experiments are performed in the Robotics Lab at the Department of Automatic Control in Lund using an ABB industrial robot Irb 2000 (Fig. 5). The controller is implemented in Matlab/Simulink, compiled and dynamically linked to the Open Robot Control System [18]. The forces are measured using a wrist-mounted, DSP-based force/torque sensor from JR3.

The physical constraint is represented by a vertical screen as seen in Fig. 5, and the impedance is controlled perpendicular to this screen using joint one, i.e., the base joint, of the robot. The situation can be modeled as in Fig. 6, where x_c is the location of the screen, x_∞ the stationary position, and x_r the desired position in the case of unconstrained motion. In the following x_r is zero. The stationary position will depend on the relation between the environmental stiffness and the robot stiffness as specified by the impedance relation. If the robot is made very stiff, then x_∞ will be close to x_r, whereas a stiff environment will lead to x_∞ being close to x_c.

The contact force was modeled as a regular spring, i.e.,

$$F = \begin{cases} 0 & x \le x_c, \\ k \cdot (x - x_c) & x > x_c. \end{cases} \tag{12}$$

The stiffness, k, of the screen used in the experiments was 5 N/rad. The position measurement was given in radians on the motor side, and using the gear ratio of -71.44 the actual values of the robot arm were computed.

V. Modeling

A good model of the base joint is needed in order to design the observer. This model is obtained by system identification. The joint is modeled as two rotating masses connected by a spring-damper, reflecting the flexibility of the gear-box and the axis (Fig. 7). The angular position and velocity on the motor side are denoted φ_1 and ω_1, whereas φ_2 and ω_2 denote the corresponding quantities of the robot arm. The process input is the torque, τ, applied by the motor and the measured process output is the angular position on the motor side, φ_1. By introducing the state variables

$$x_1 = \varphi_1, \quad x_2 = \omega_1, \quad x_3 = \varphi_2, \quad x_4 = \omega_2 \tag{13}$$

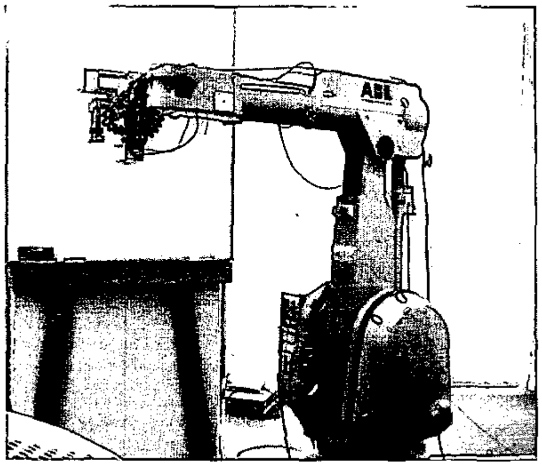

Fig. 5. The experimental setup. An ABB industrial robot Irb 2000 with an open control system is used, and the impedance control is performed perpendicular to the screen. The base joint (joint one) of the robot was used.

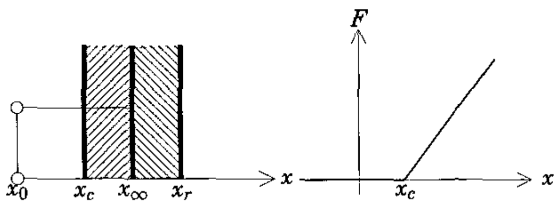

Fig. 6. A screen representing a physical constraint. x_c is the location of the screen, x_∞ the stationary position, and x_r the desired position in the case of unconstrained motion (*left*). The contact force nonlinearity (*right*): When the robot is in contact with the environment, the force can be modeled as a linear spring, the force being zero without contact.

and the input $u(t) = \tau(t)$, the system can be written on state-space form as

$$\begin{aligned} \dot{x} &= \begin{bmatrix} 0 & 1 & 0 & 0 \\ -\frac{k_{12}}{J_1} & -\frac{D_1+d_{12}}{J_1} & \frac{k_{12}}{J_1} & \frac{d_{12}}{J_1} \\ 0 & 0 & 0 & 1 \\ \frac{k_{12}}{J_2} & \frac{d_{12}}{J_2} & -\frac{k_{12}}{J_2} & -\frac{D_2+d_{12}}{J_2} \end{bmatrix} x + \begin{bmatrix} 0 \\ \frac{1}{J_1} \\ 0 \\ 0 \end{bmatrix} u \\ y &= \begin{bmatrix} 1 & 0 & 0 & 0 \end{bmatrix} x(t) \end{aligned} \tag{14}$$

The numerical values of the coefficients in the state-space model above are estimated by *prediction error method* in Matlab [16]. The final identified model is given by

$$\begin{aligned} \dot{x} &= \begin{bmatrix} 0 & 1 & 0 & 0 \\ -11476 & -8 & 11476 & 2 \\ 0 & 0 & 0 & 1 \\ 8445 & 2 & -8445 & -9 \end{bmatrix} x + \begin{bmatrix} 0 \\ 700 \\ 0 \\ 0 \end{bmatrix} u \\ y &= \begin{bmatrix} 1 & 0 & 0 & 0 \end{bmatrix} x \end{aligned} \tag{15}$$

Model validation is shown in Fig. 8 comparing true process output with a simulation of the state-space model (15).

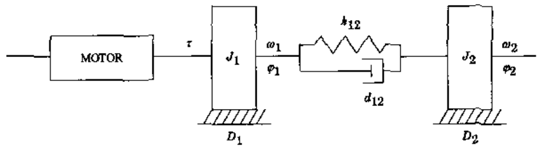

Fig. 7. Physical model of the robot joint. The angular position on the motor side, φ_1, is measurable. The input is the torque, τ, actuated by the motor.

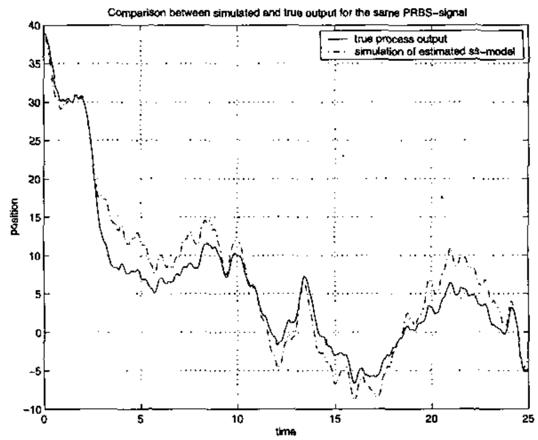

Fig. 8. Comparison of true process output with a simulation of the estimated state-space model. The same PRBS-signal has been used as input in both cases.

VI. Simulations and Experiment

The dash-dotted curve in Fig. 3 shows a simulation using the design in the example above. The dashed line in the position plot marks the location of the screen. By modifying the penalty K_p the stiffness of the impedance relation is changed, which is shown by the solid line. Fig. 4 shows a simulation examining the influence of the penalty D_p. It is seen that the damping during the transient is affected, but that the stationary force is the same in both cases. The simulations were done in Matlab/Simulink.

An experiment on the real robot is shown in Fig. 9. This experiment corresponds to the case analyzed in the example, and is the same as the dash-dotted curve in the simulation in Fig. 3. The initial force transient before contact is an inertia force. The correspondence between experiment and simulation is good. As predicted in the analysis, stability is preserved at contact.

VII. Discussion

Recently, it has been shown that relaxation of the controllability and observability conditions imposed in the

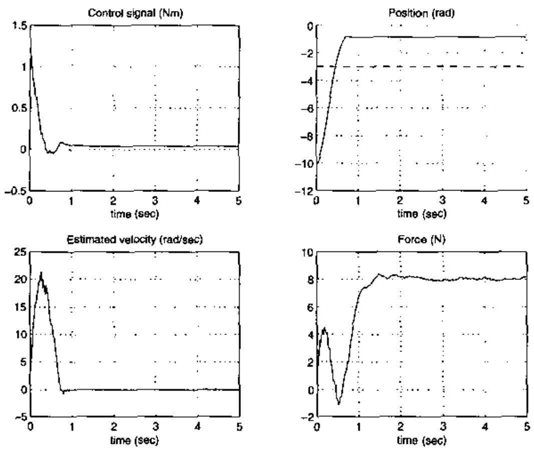

Fig. 9. Experiment of observer-based impedance control corresponding to the design analyzed in the example, i.e., $K_p = 10$ and $D_p = 1$. The initial force transient before contact is an inertia force. The dashed line in the position plot marks the location of the screen.

Yakubovich-Kalman-Popov (YKP) lemma can be made for a class of nonlinear systems described by a linear time-invariant system (LTI) with a feedback-connected cone-bounded nonlinear element [12]. This approach was used in order to achieve robustness in impedance control design.

An obvious extension would be to apply the results to full-dimensional wrenches. This would include use of the Jacobian to translate forces from the task space to the operational space, as well as full dynamics for the robot and gravity compensation. The simple linear model of the robot would not be sufficient and the coupling between the links would require nonlinear observer-based control [19]. Another possible extension would be to apply the results on other force control schemes such as parallel force/position control or hybrid force/position control [2], [5], [6], [21].

The approach to modification of the relative-degree and SPR properties is related to the 'parallel feedforward' as proposed in the context of adaptive control [1]. Another related idea is passification by means of shunting introduced by Fradkov [4]. All these approaches represent derivation of a loop-transfer function with SPR properties for a control object without SPR properties by means of dynamic extensions or observers. This idea that combines attractively with the observer-based SPR design used here. The Bar-Kana approach [1] starts with the following transfer functions

$$
\begin{aligned}
G_0(s), G_R(s), \quad &\Rightarrow \quad G_{cl}(s) = \frac{G_0(s)}{1+G_R(s)G_0(s)} \\
G_1(s) \quad &= \quad G_0(s) + \frac{1}{G_R(s)} \qquad (16)
\end{aligned}
$$

Assuming that some $G_R(s)$—not necessarily proper or implementable control transfer function such as $(K + sD)$—would provide stabilizing SPR feedback control when feedback interconnected with $G_0(s)$, then a stable feedback loop can be closed around $G_1(s)$ of Eq. (16). The key observation is that the implementable 'parallel feedforward' transfer function

$$
G_P(s) = \frac{1}{G_R(s)} \qquad (17)
$$

will achieve stable feedback without differentiation. Design of a mechanical device based on a related idea of impedance matching has been suggested by Dohring and Newman [3]. Combination of the 'parallel feedforward' [1] and the SPR design [12] may further increase robustness properties.

VIII. Conclusions

An approach to observer-based impedance control in one dimension has been presented. Impedance control is a robot force control technique aimed at control of the relation between position and force, rather than force control or position control separately. This technique has proved useful in dealing with geometric uncertainty, i.e., when the exact location of the environment is unknown. As industrial robots are often equipped with position sensors only, the velocity had to be reconstructed. A full-order observer was used to estimate the velocity, and the model of the robot joint needed for the observer dynamics was obtained by system identification.

The approach taken, observer-based impedance control, was based on results impedance control combined with observer-based SPR feedback [9], [12]. The design included the solution of a Riccati equation, and the stiffness and damping in the impedance relation were modified by the choice of weights in the design matrix. Stability was proven by means of a modified Popov criterion. The theoretical results were verified by simulations and experiments, the experiments being carried out on an ABB industrial robot Irb 2000.

IX. References

[1] I. Bar-Kana. Parallel feedforward and simplified adaptive control. *Int J. Adaptive Control and Signal Processing*, 1:95–109, 1987.

[2] S. Chiaverini, B. Siciliano, and L. Villani. A survey of robot interaction control schemes with experimental comparison. *IEEE/ASME Trans. Mechatronics*, 4:273–285, 1999.

[3] M. Dohring and W. Newman. Admittance enhancement in force feedback of dynamic systems. In *Proc. 2002 IEEE Int. Conf. Robotics and Automation*, pages 638–643, Washington, DC, May 2002.

[4] A. Fradkov. Nonlinear feedback control: Regulation, tracking, oscillations. In *1st IFAC Workshop on New Trends in Control Systems Design*, pages 426–431, Smolenice, 1994.

[5] D.M. Gorinevsky, A.M. Formalsky, and A.Y. Schneider. *Force Control of Robotics Systems*. CRC Press, New York, 1997.

[6] A. Hemami and G. Zeng. An overview of robot force control. *Robotica*, 15:473–482, 1997.

[7] D. Henriksson. Observer-based impedance control in robotics. Master's thesis, Dept. Automatic Control, Lund University, 2000.

[8] D. Henriksson, R. Johansson, and A. Robertsson. Observer-based impedance control in robotics. In *Proc. 5th IFAC Symp. Nonlinear Control Systems (NOLCOS 2001)*, pages 360–365, St. Petersburg, Russia, July 4-6 2001.

[9] N. Hogan. Impedance control: An approach to manipulation, Parts I-III. *J. Dynamic Systems, Measurement, and Control, ASME*, 107:1–24, 1985.

[10] R. Johansson. *System Modeling and Identification*. Prentice Hall, Englewood Cliffs, NJ, 1993.

[11] R. Johansson and A. Robertsson. Observer-based SPR feedback control system design. 5th IFAC Symp. Nonlinear Control Systems (NOLCOS 2001), St. Petersburg, Russia, 2001.

[12] R. Johansson and A. Robertsson. Observer-based strict positive real (SPR) feedback control systems design. *Automatica*, 38:1557–1564, 2002.

[13] R. Johansson and M.W. Spong. Quadratic optimization of impedance control. In *Proc. IEEE Conf. Robotics and Automation*, pages 616–621, San Diego, CA, 1994.

[14] H.K. Khalil. *Nonlinear Systems*. Prentice-Hall, Upper Saddle River, NJ, 2nd edition, 1996.

[15] P. V. Kokotović and H. J. Sussman. A positive real condition for global stabilization of nonlinear systems. *Systems and Control Letters*, 13:125–133, 1989.

[16] L. Ljung. *System Identification Toolbox; User's Guide*. The MathWorks Inc., Natick, MA, 1991.

[17] P. Molander and J.C. Willems. Synthesis of state feedback control laws with a specified gain and phase margin. *IEEE Trans. Automatic Control*, AC-25:928–931, 1980.

[18] K. Nilsson and R. Johansson. Integrated architecture for industrial robot programming and control. *J. Robotics and Autonomous Systems*, 29:205–226, 1999.

[19] A. Robertsson. *On Observer-Based Control of Nonlinear Systems*. PhD thesis, Dept. Automatic Control, Lund Inst. Tech., 1999.

[20] B. Siciliano and L. Villani. Parallel force/position controller with observer for robot manipulators. In *Proc. 36th Conf. Decision and Control*, pages 1335–1340, 1997.

[21] B. Siciliano and L. Villani. *Robot Force Control*. Kluwer Academic Publishers, Dordrecht, NL, 1999.

Acknowledgement: The authors thank Dan Henriksson, M. Sc., for the contributions made during his master thesis project [7].

This research was sponsored by Nutek under the research program 'Complex Technical Systems'.